Blade Contour Deformation and Helicopter Performance

Mark E. Calvert,* Tin-Chee Wong† and James A. O'Malley, III.‡
Aviation and Missile Research, Development and Engineering Center,
U.S. Army Research, Development and Engineering Command,
Redstone Arsenal, AL, 35898-5000.

The United States Army helicopter fleet is experiencing deformation of rotor blade contours from sand erosion and the implementation of technologies to reduce it. An investigation was performed to determine the effect of these types of degradations on the tail rotor performance of Apache attack helicopters. Computational fluid dynamics was used to calculate aerodynamic coefficients for representative deformed airfoil sections. A hover analysis code was used to evaluate the impact of the damaged airfoils on the tail rotor performance. The results show that airfoil erosion can lead to a significant reduction in the maximum thrust available from worn tail rotors.

Nomenclature

c	=	chord length, ft.
c_d	=	section drag coefficient
CFD	=	computational fluid dynamics
c_l	=	section lift coefficient
C_P	=	power coefficient
C_T	=	thrust coefficient
DOD	=	Department of Defense
FM	=	figure of merit
NACA	=	National Advisory Committee on Aeronautics
PA	=	pressure altitude (ft.)
R	=	rotor radius
SLS	=	sea level standard atmospheric conditions
U.S.	=	United States
α	=	angle of attack, deg.

I. Introduction

Recent operations in the desert terrain of Southwest Asia has increased U. S. Army interest in the effect of sand erosion on helicopter rotors. Rotor blade replacement represents a significant cost over a helicopter's operational life. This expense results from both the price of replacement articles and the logistical and operational cost of blade replacement on helicopters deployed in the field. These costs are exacerbated by the increased operational tempo under which helicopters are now being used.

Most helicopter rotor blades include erosion protection in the form of leading edge strips made from metals such as nickel, titanium and stainless steel. Polyurethane-based coatings, tapes and boots have also been used for erosion protection. However, neither strategy gives optimal erosion resistance from both rain and sand. Metal leading edges have excellent rain resistance but poor sand erosion performance. Conversely, polyurethane-based coatings have good sand erosion protection, but poor rain resistance. Ultimately, all erosion protection systems utilize sacrificial materials, resulting in continually changing airfoil section contours. Application of the rotor protection products can

* Aerospace Engineer, Aviation Engineering Directorate, AMSRD-AMR-AE-A, Member AIAA.
† Aerospace Engineer, Aviation Engineering Directorate, AMSRD-AMR-AE-A.
‡ Chief Engineer, Aviation Engineering Directorate, AMSRD-AMR-AE-A, Member AIAA.

also cause additional changes in the contour of the rotor blade. Thus, most helicopters in the field operate with off-design blade contours.

The National Advisory Committee on Aeronautics (NACA) conducted several studies of the influence of airfoil contour variation on aerodynamic performance during the 1930's and 40's. Ward[1] investigated the effect of minor contour variation on airfoil aerodynamic performance. Ward compared two version of the Göttingen 387 airfoil, one constructed from ordinates from the Göttingen laboratory (Göttingen 387-G), and one constructed from ordinates from NACA (Göttingen 387). The variation between the two profiles was within one-half percent of the chord length. Results from wind tunnel tests showed a 4.5 percent difference in maximum lift, an 8.0 percent difference in minimum profile drag, and a 3.5 percent difference in the lift-to-drag ratio. Ward also compared the NACA 100 and the NACA 0021 symmetrical airfoils as representative of the difference observed between airfoil ordinates from different laboratories. For this case, the physical variation between the two airfoil sections was less than one-quarter percent of the chord length. The wind tunnel tests showed a 9.4 percent difference in maximum lift and a 2.3 percent difference in the lift-to-drag ratio.

In 1934, Jacobs[2] investigated the effects of protuberance on airfoil section aerodynamic coefficients. He found that protuberances as small as one thousandth of the chord length forward of the maximum thickness location could cause a significant increase in airfoil drag. Fairing was found to reduce the drag, but did not eliminate the increased drag. The maximum airfoil lift coefficient was also found to be significantly reduced by protuberances of the size of a typical aircraft wing's surface roughness. Jacobs[3] extended his research to include the effect of protuberances on wings. He found that protuberance of short span could cause a reduction in a wing's maximum lift, but that fairing the protuberances could mitigate this effect.

Other researchers[4,5,6] have investigated the effects of environmental roughness on airfoil aerodynamic performance. These effects include rain, insect deposits and ice accretion. Wetted airfoils have been shown to have a 30 percent reduction in lift for torrential rain conditions. Insect impacts on airfoil sections can act as distributed roughness. The equivalent sand roughness of the surface is dependent on the predominant species of insect, and the speed at which insects impact the airfoil. The effect of ice accretion is dependent on the thickness of the ice on the airfoil. The predominant results of these investigations are that even minor variation in airfoil surface contour within the leading 5 percent of the chord length can cause significant changes in aerodynamic performance, areas that will typically encounter the greatest sand erosion.

II. Airfoil Contour Degradation and Aerodynamic Performance

The AH-64 Apache Attack Helicopter tail rotor blade consists of a modified NACA 63-414 airfoil[7,8,9] with an additional 10 percent 6^o trailing edge tab for the tail rotor.[8] The addition of the tab reduces the airfoil maximum thickness ratio from 14 percent to 12.8 percent of the total chord length. For this investigation, the most critical performance of the tail rotor is expected to occur when the helicopter is in hover. The vertical tail does not generate any aerodynamic forces to offset the torque generated by the main rotor. The vertical tail also introduces blockage effects that the tail rotor must overcome.

Figure 1 shows a plot of the baseline and damaged airfoil sections. As may be seen from the figure, the greatest deviation occurs on the upper surface between 5 percent and 35 percent of the chord length. This deviation reaches a maximum of approximately 5 percent of the total chord length at 16 percent chord. Another significant deviation occurs on the lower surface between 8 percent and 22 percent of the chord length. This deviation reaches a maximum of approximately 2 percent of the total chord at the 15 percent chord location. There are additional deviations along the 70 percent trailing length of the airfoil; however, a portion of this deviation may be the result of the transformation operations used to align the measured airfoil ordinates with the ideal baseline ordinates. In any case, previous research has shown that aerodynamic behavior is influenced the most by the leading edge airfoil contour.

Figure 2 shows the unstructured grids for the baseline and damaged airfoils. The unstructured Navier-Stokes solver FUN2D was used for the CFD simulations. This flow solver has been developed and supported by the NASA Langley Research Center. The code[10] uses an implicit, upwind, finite-volume discretization in which the dependent variables are stored as mesh vertices. Inviscid fluxes at cell interfaces are computed using the flux-differencing scheme of Roe and viscous fluxes are evaluated by using an approach equivalent to a central-difference Galerkin procedure. For steady-state flows, temporal discretization is performed by using a backward Euler time-stepping scheme. At each time step, the linear system of equations is approximately solved with an implicit line relaxation scheme. A local time-step technique is employed to accelerate convergence to steady-state solution. For all results presented in this paper, the one-equation model of Spalart and Allmaras is employed and solved in a loosely coupled fashion.

The Apache tail rotor tip speed is 680 ft/sec. The speed at the root cutout is 223 ft/sec. For the operational environments studied in this investigation, the tail rotor in hover operates within the range of Mach numbers between 0.2 at the root cutout to 0.6 at the rotor tip. Based upon this information, CFD solutions were run for the Mach numbers of 0.3, 0.4, 0.5 and 0.6, with the corresponding Reynolds numbers of 2.1 x 10^6, 2.8 x 10^6, 3.5 x 10^6 and 4.3 x 10^6, respectively. The 0.3 Mach results were assumed to approximate lower Mach number results. Nondimensional lift and drag coefficients are shown in Figures 3 through 6. Grid independence for these solutions was checked by doubling the number of grid points on the airfoil surface and checking for converged lift and drag coefficients.

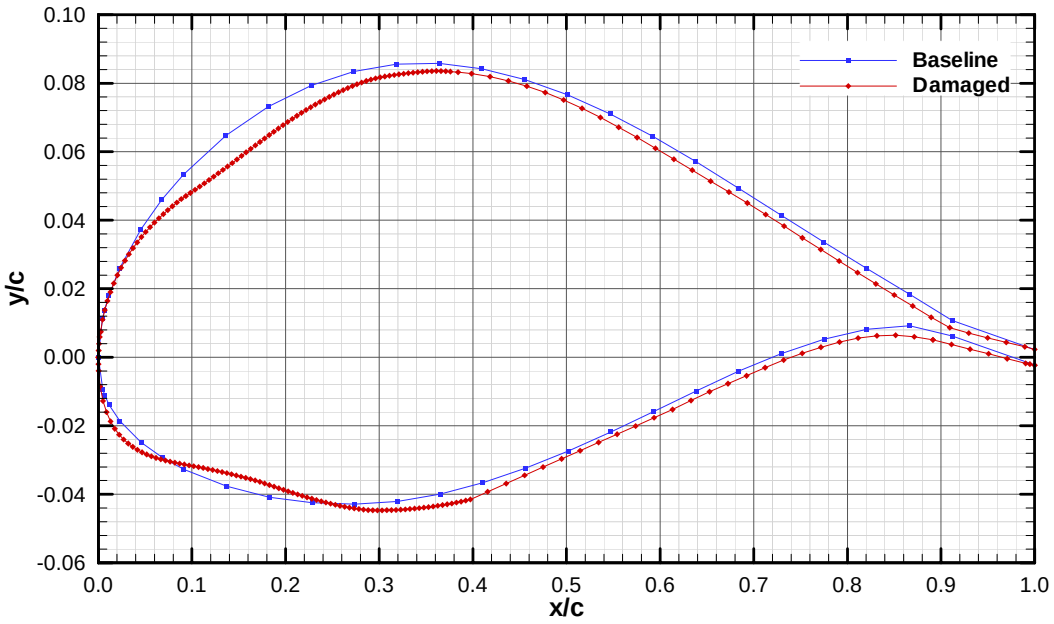

Figure 1 Whale plot of the baseline and damaged airfoil sections.

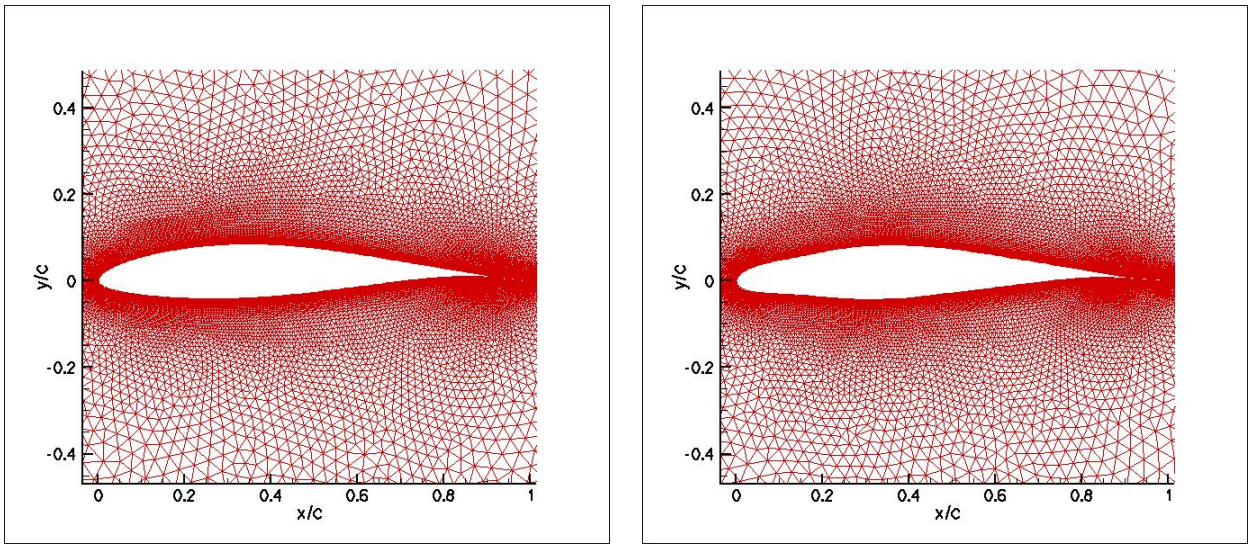

Figure 2 Unstructured meshes for baseline (left) and damaged (right) airfoils.

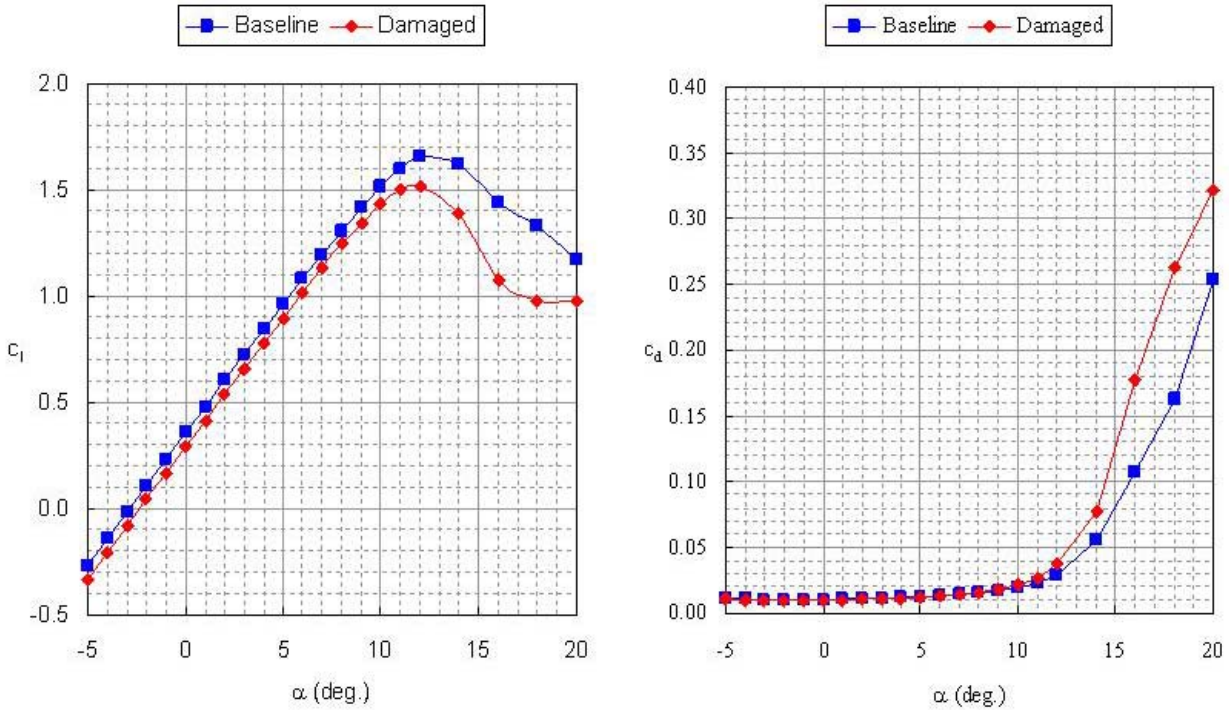

Figure 3 Lift and drag coefficients for Mach number 0.3.

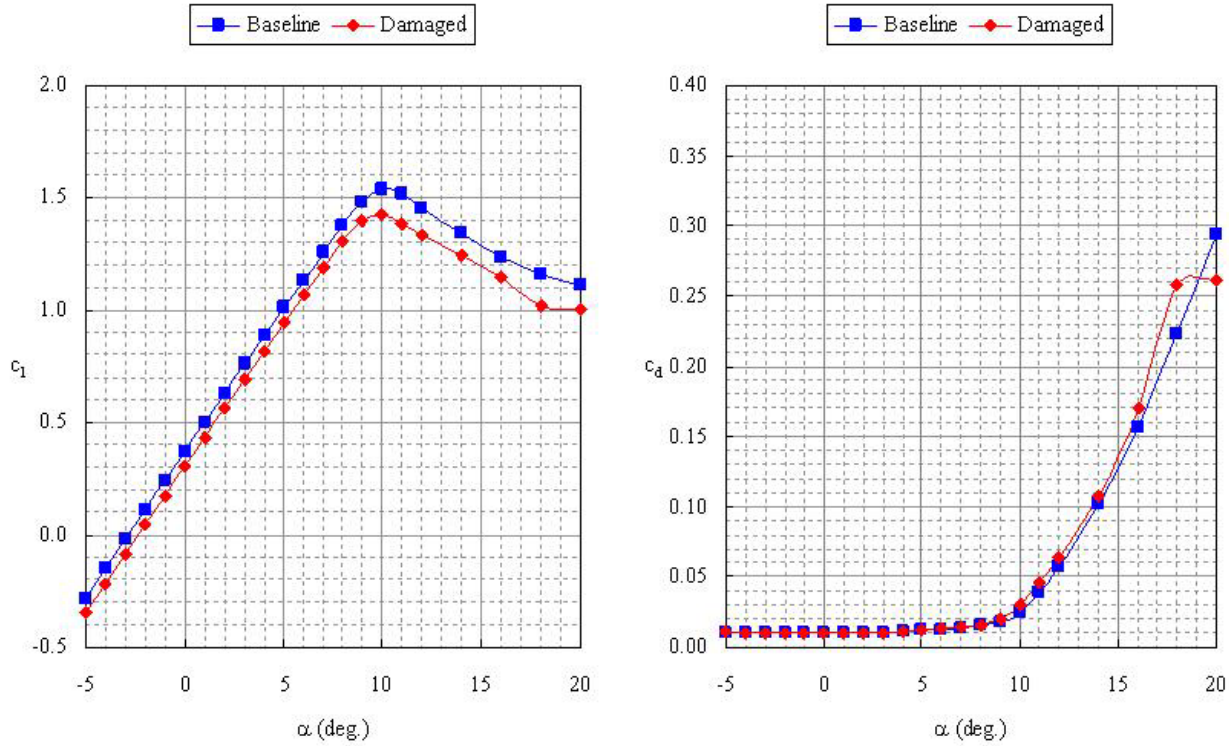

Figure 4. Lift and drag coefficients for Mach number 0.4.

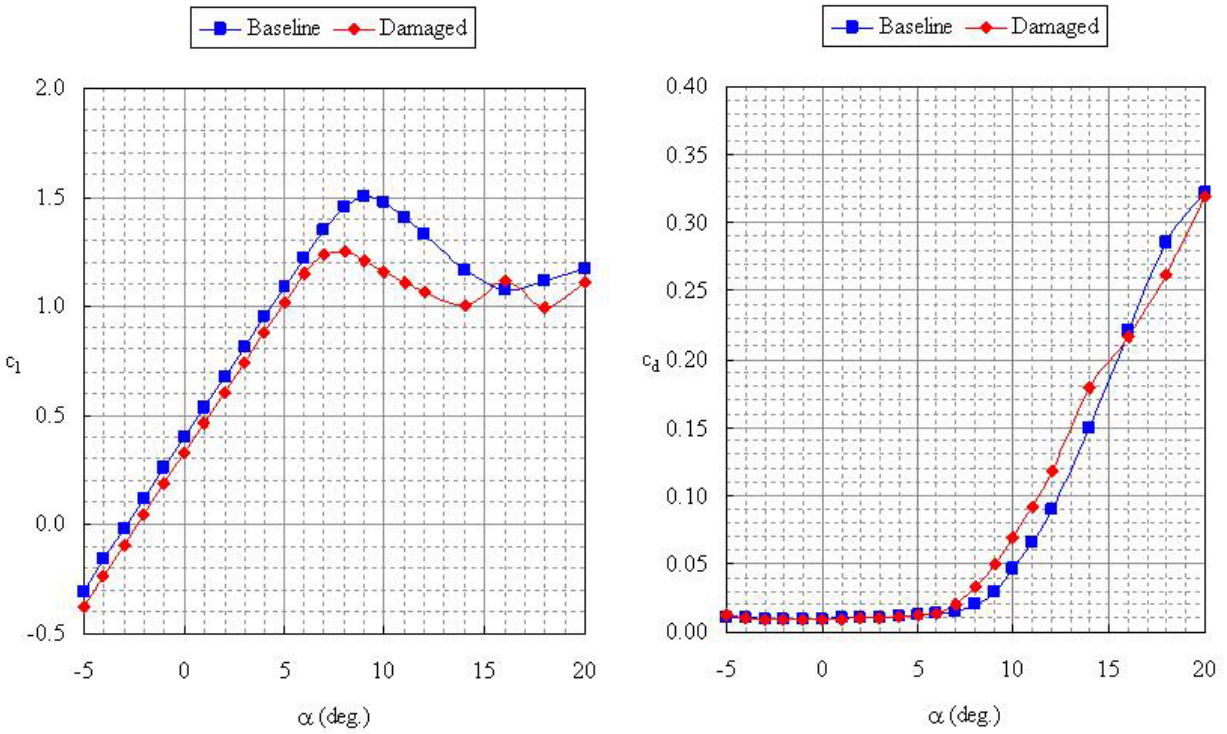

Figure 5 Lift and drag coefficients for Mach number 0.5.

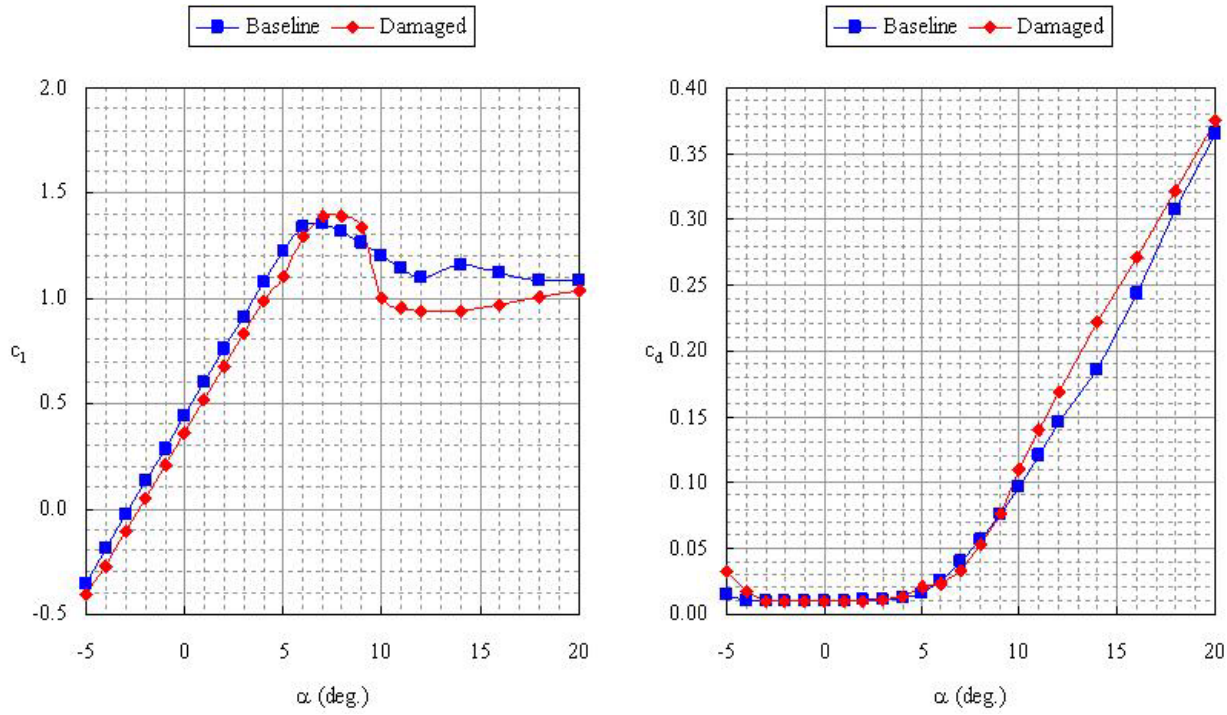

Figure 6 Lift and drag coefficients for Mach number 0.6.

As may be seen from the figures, the lift coefficient solutions within the linear region are slightly biased for the damaged airfoils. This bias indicates the possibility of a chordline angular difference between the two profiles. Figure 1 shows that the profiles were referenced to the trailing edge (actual measurements in the field). The drag coefficients at small angles of attack are not significantly different for the cases shown. The uniformity of the lift

coefficient bias, and the lack of a significant difference in drag coefficients across all of the Mach numbers for the small angles of attack would seem to confirm that this difference in caused by a geometrical orientation problem, rather than airfoil damage.

All of the Mach number cases reveal differences between the damaged contour and the baseline for the regions approaching maximum stall. However, the differences between baseline and stall do not change in a recognizable manner as a function of Mach number. The 0.5 Mach number case has the largest decrease in maximum lift coefficient for the damaged airfoil as compared to the baseline case. However, the 0.6 Mach number case shows the damaged airfoil having a larger maximum lift coefficient than the baseline case. The drag coefficient results reveal that the damaged airfoil produces greater drag than the baseline airfoil over some of the larger angles of attack range. However, there are areas where the difference in drag is inconclusive. Both lift and drag coefficient results show that the damaged airfoil goes into a deeper stall than the baseline airfoil.

These results indicate that erosion and damage to tail rotors can significantly affect airfoil aerodynamic performance. However, there is *not* a definitive trend that would allow rule-of-thumb estimates for degradation in tail rotor performance.

III. Degraded Rotor Contours on Tail Rotor Performance

In order to evaluate the effect of the damaged airfoils on the Apache tail rotor performance, a hover analysis was conducted using the LSAF hover analysis code.[11-14] LSAF is based on a circulation coupled prescribed wake to calculate the velocity field within the rotor wake in order to determine the induced velocity at the rotor blade. LSAF uses a lifting surface method to calculate the lift generated by a rotor. A strip-analysis combined with an airfoil table look-up is used to determine the aerodynamic drag. LSAF has been shown to accurately predict the hover performance over a wide range of conditions and thrust levels for a variety of isolated rotors and rotorcraft[12]. For the Apache tail rotor, the hover capability was evaluated at two flight conditions: standard sea-level temperature and pressure, denoted as SLS, and for a pressure altitude of 6,000 feet and 95 degrees Fahrenheit, denoted as 6K/95-deg. Relevant properties for these conditions are given in Table 1. Geometric properties for the Apache tail rotor blade used in the LSAF calculations are given in Table 2.

Airfoil tables for both the baseline and damaged airfoils were created. The data shown in Figures 4 through 6 were merged into an existing NACA 0012 airfoil table. The new airfoil data was faired into the existing airfoil data in an effort to eliminate sharp jumps.

Figure 7 shows nondimensional tail rotor thrust as a function of nondimensional power. Figure 8 shows thrust as a function of tail rotor pitch for the standard sea level condition and 6,000 ft. PA/ 95^{o} Fahrenheit. The vertical black lines show the helicopter pilot's pedal limits for the tail rotor collective; the left pedal is used to turn left, and the right pedal is used to turn right. Both plots show a small reduction in thrust from the damaged blade as compared to the ideal (baseline) blade for most of the operational range. As noted previously, the difference for the lower angles of attack may be due to discrepancies in aligning the blade contours, as shown in Figure 1. A more significant feature of both plots shows that the damaged tail rotor blades will stall within the pedal limits for both atmospheric conditions whereas the baseline profile does not.

The data shown on the plots are direct output from the LSAF calculations for very small collective pitch increments. The variance shown at the high pitch angles near stall and at low thrust and negative thrust conditions indicates some disagreement among the many convergence requirements. The main convergence requirements include: lift curve slope, tip vortex rollup, and rotor wake element (inboard wake sheet and tip vortex) displacement rates. Even though there are some problems with the convergence, the calculated trend is an accurate representation of the static stall limits and the low thrust and negative thrust capabilities of a rotor. No other rotor aerodynamic analytical method with the LSAF level of flow assumptions is capable of such a complete evaluation.

Figure 9 shows rotor figure of merit as a function of thrust coefficient. The damaged rotor has a better efficiency for the negative thrust levels. The efficiency levels are close for the positive thrust levels, until the damaged rotor stalls. Presenting rotor performance in such a way accentuates the differences.

Table 1. Atmospheric properties.

	SLS	6K/95-deg.
Temperature (^{o}F)	59	95
Pressure Altitude (ft.)	0	6,000
Density (slugs/ft^{3})	2.38 x 10^{-3}	1.78 x 10^{-3}
Speed of Sound (ft/sec.)	1,116	1,155

Table 2. Apache tail rotor properties.

Rotor tip speed (ft./sec)	680
Rotor radius (ft)	4.5833
Root cutout (ft.)	1.5
Chord (ft.)	0.8333
Twist (deg.)	-8

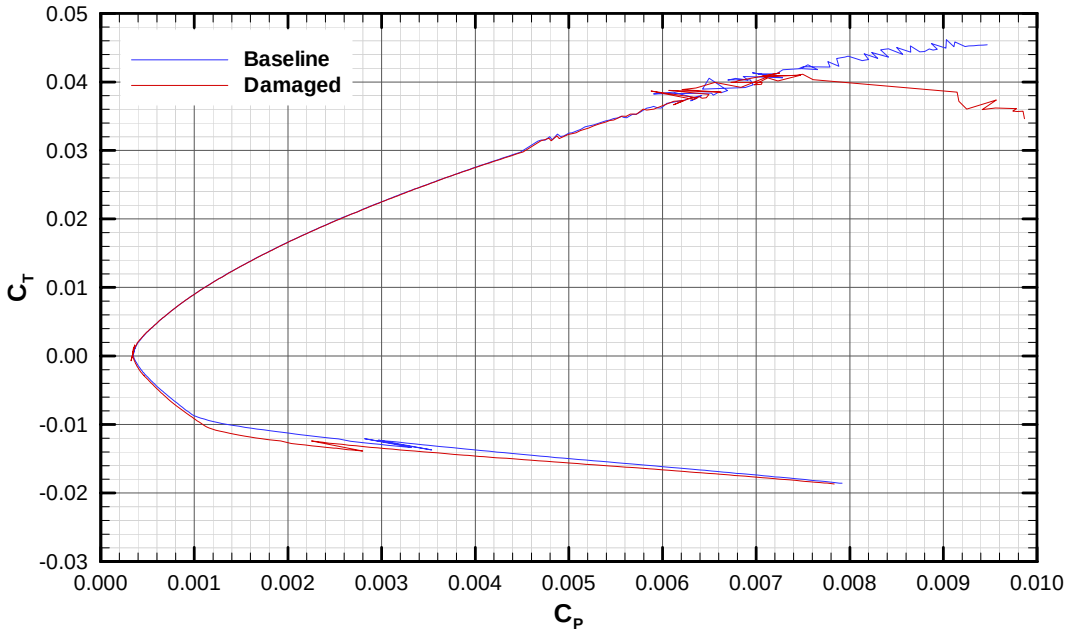

Figure 7. Thrust coefficient versus power coefficient.

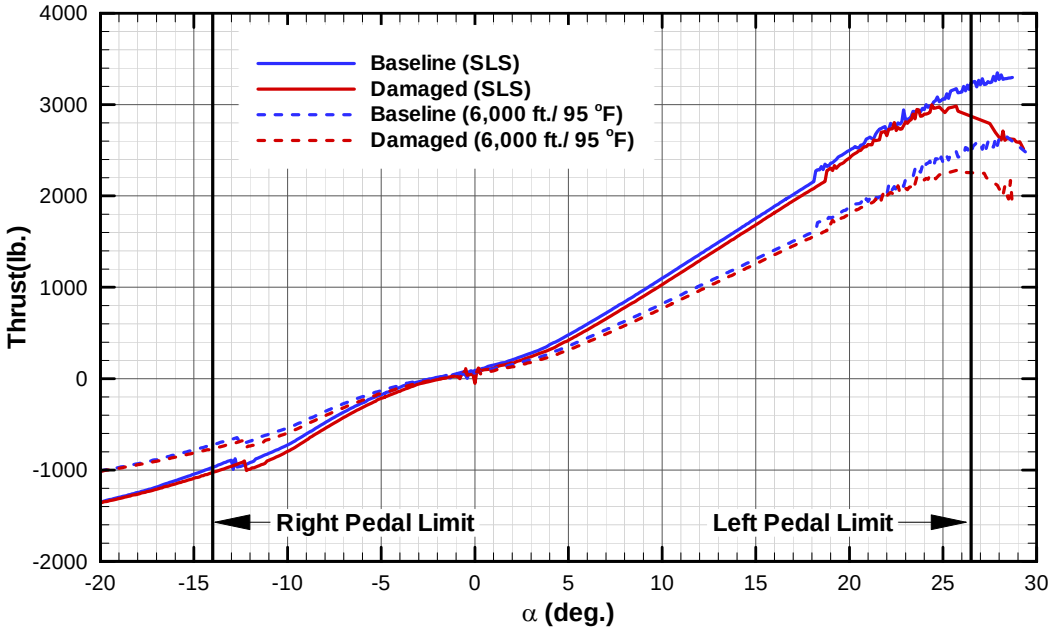

Figure 8. Thrust versus blade pitch.

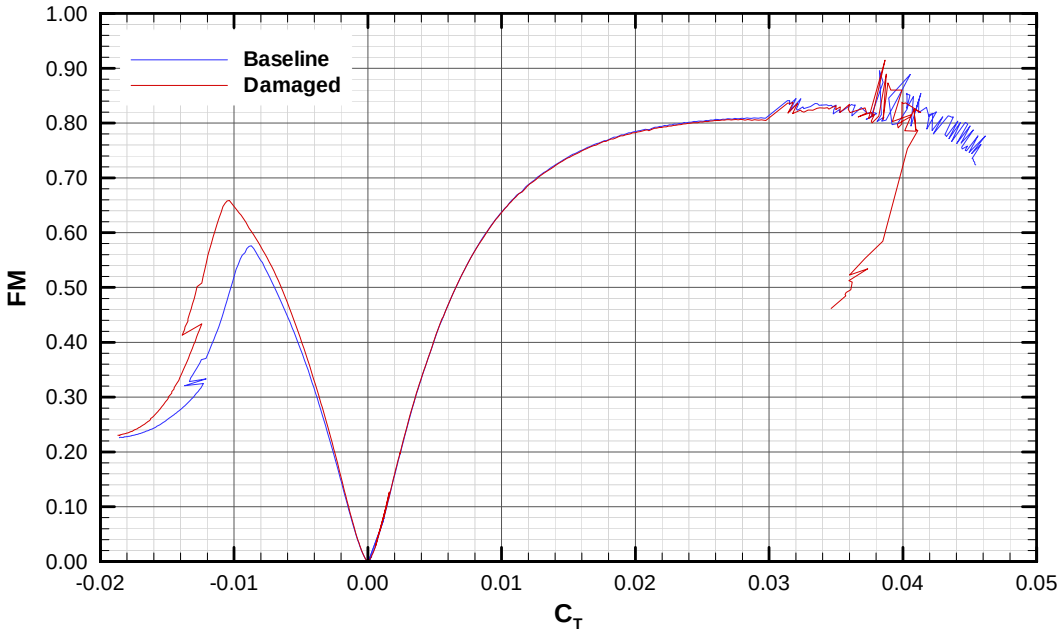

Figure 9. Figure of merit versus thrust coefficient.

IV. Conclusion

It is possible to quantify helicopter performance degradation due to rotor blade degradation from wear and repair. Computational fluid dynamics may be used to generate (or to revise existing) aerodynamic coefficient tables for deformed airfoils. These revised tables may then be used in performance analysis codes to determine the differences between baseline and deformed rotor blade performance. Results for the case considered shows that the greatest impact is earlier stall for the damaged blades. Additional research is needed to quantify the general sensitivity of rotor blade performance to small deformations near the leading edge region.

Acknowledgments

This work was supported in part by a grant of computer time from the Department of Defense High Performance Computing Modernization Program at the Aeronautical Systems Center Major Shared Resource Center, the Army Research Laboratory Major Shared Resource Center, the Engineer Research and Development Center Major Shared Resource Center, the Naval Oceanographic Office Major Shared Resource Center, and the Space and Missile Defense Command Simulation Center and Advanced Research Center Allocated Distributed Center.

References

[1]Ward, K. E., “The Effect of Small Variations in Profile of Airfoils,” NACA TN 361, 1931.

[2]Jacobs, E. N., "Airfoil Section Characteristics as Affected by Protuberances," NACA TR 446, 1934.

[3]Jacobs, E. N., and Sherman, A., "Wing Characteristics as Affected by Protuberances of Short Span," NACA TR 449, 1934.

[4]Cebici, T., “Effects of Environmentally Imposed Roughness on Airfoil Performance,” NASA CR-179639, 1987.

[5]Wilder, M. C., “Control of Unsteady, Separated Flow Associated with the Dynamic Stall of Airfoils,” NASA-CR-198972, 1995.

[6]Matheis, B. D., Huebsch, W. W., and Rothmayer, A. P., “Separation and Unsteady Vortex Shedding from Leading Edge Surface Roughness,” ADM201868, 2004.

[7]Patterson, E. W., and Braslow, A. L., “Ordinates And Theoretical Pressure-Distribution Data for NACA 6- and 6a-Series Airfoil Sections with Thicknesses from 2 to 21 and from 2 to 15 Percent Chord, Respectively,” NACA TN 4322, 1958.

[8]Stivers, L. S., “Effects of Subsonic Mach Number on the Forces and Pressure Distributions on Four NACA 64A-Series Airfoil Sections at Angles of Attack as High as 28°.” NACA-TN-3162, 1954.

[9]Amer, K. B., and Prouty, R. W., “Technology Advances in the AH-64 Apache Advanced Attack Helicopter,” *39th Annual Forum Proceedings*, American Helicopter Society, Alexandria, VA, 1983, pp. 550-568.

[10]Anderson, W. K., and Bonhaus, D. L., "An Implicit Upwind Algorithm for Computing Turbulent Flows on Unstructured Grids," *Computers and Fluids*, Vol. 23, No. 1. pp. 1-21, 1994.

[11]LSAF, Lifting Surface Aerodynamics and Performance Analysis of Rotors in Axial Flight, Software Package, Ver. 2.XX, Computational Methodology Associates, Colleyville, TX. 2003.

[12]Kocurek, J. D., Berkowitz, L. F., and Harris, F. D., "Hover Performance Methodology at Bell Helicopter Textron," Preprint No. 80-3, *36th Annual Forum Proceedings*, American Helicopter Society, Washington, D. C., 1980.

[13]Kocurek, J. D., "A Lifting Surface Performance Analysis with Wake Circulation Coupled Wake for Advanced Configuration Hovering Rotors," Ph.D. Dissertation, Dept. of Aerospace Engineering, Texas A&M University, College Station, TX, 1978.

[14]Kocurek, J. D., and Tangler, J. L., "A Prescribed Wake Lifting Surface Hover Performance Analysis," *Journal of the American Helicopter Society*, Vol. 22, No. 1, 1977, pp. 24-35.